



Published in final edited form as:

J Control Release. 2016 December 28; 244(Pt A): 1–13. doi:10.1016/j.jconrel.2016.10.026.

Single ocular injection of a sustained-release *anti*-VEGF delivers 6 months pharmacokinetics and efficacy in a primate laser CNV model

Peter Adamson^{a,i}, Thomas Wilde^{b,i}, Eric Dobrzynski^{b,i}, Caroline Sychterz^{b,i}, Rodd Polsky^{c,i}, Edit Kurali^{d,i}, Richard Haworth^{c,j}, Chi-Man Tang^{e,k}, Justyna Korczynska^{f,k}, Fiona Cook^{f,k}, Irene Papanicolaou^{e,k}, Lemy Tsikna^{f,k}, Chris Roberts^{f,k}, Zoe Hughes-Thomas^{f,k}, James Walford^{g,k}, Daniel Gibson^{g,k}, John Warrack^{h,k}, Jos Smal^l, Ruud Verrijk^l, Paul E. Miller^m, T. Michael Nork^{m,n}, Jeffery Prusakiewicz^o, Timothy Streit^o, Steven Sorden^o, Craig Struble^o, Brian Christian^o, and Ian R. Catchpole^{a,e,k,*}

^aGSK Ophthalmology ^bDrug Metabolism & Pharmacokinetics ^cSafety Assessment ^dTarget Science Statistics ^eBioPharm Innovation ^fBioPharm Discovery ^gBioPharm Process Research ^hAnalytical Sciences ⁱGSK, King of Prussia, PA, USA ^jGSK Ware, UK ^kGSK Medicines Research Centre, Stevenage, UK ^lOctoPlus NV, Leiden, The Netherlands ^mOSOD, Madison, WI, USA ⁿUniversity of Wisconsin School of Medicine and Public Health, Madison, WI, USA ^oCovance, Madison, WI, USA

Abstract

A potent *anti*-vascular endothelial growth factor (VEGF) biologic and a compatible delivery system were co-evaluated for protection against wet age-related macular degeneration (AMD) over a 6month period following a single intravitreal (IVT) injection. The *anti*-VEGF molecule is dimeric, containing two different anti-VEGF domain antibodies (dAb) attached to a human IgG1 Fc region: a dual dAb. The delivery system is based on microparticles of PolyActive™ hydrogel

This is an open access article under the CC BY-NC-ND license (<http://creativecommons.org/licenses/by-nc-nd/4.0/>).

*Corresponding author at: GSK Medicine's Research Centre, Gunnels Wood Road, Stevenage, Herts SG1 2NY, UK. ian.r.catchpole@gsk.com (I.R. Catchpole).

Author contributions: I.R.C. conceived, designed study plans, analysed, interpreted data, compiled and wrote the manuscript, P.A. funded the work, contributed to microparticle Cynomolgus PK and efficacy study designs and revised the manuscript, T.W. performed modelling, PK data analysis, interpretation and human translations, E.D. and C.S. performed Cynomolgus tissue processing, PK sample MSD analysis and data processing, R.P., ADA analysis, E.K. statistical analysis for laser CNV, R.H., animal study design and histopathology interpretation, C.M.T. developed, performed functional, integrity and RBA MSD assays, *in vitro* and rabbit, J.K., L.T., C.R., Z.H.T., and D.G. constructed expressed, purified and analysed dual dAb and intermediate molecules, F.C. directed all rabbit experiments and tissue processing, I.P. provided formulation insights for injection of particulates, Jo.Wa. analysed microparticles by SEM, J.S. and R.V. selected PolyActive polymers, formulated microparticles and performed total protein release analysis *in vitro*, P.M. and T.M.N. provided ophthalmology input, interpretation and inflammation and efficacy reports for Cynomolgus studies, J.P. & T.S. performed 6 month Cynomolgus PK and efficacy studies, respectively, S.S. performed histopathology for Cynomolgus efficacy study, C.S. and B.C. designed long term Cynomolgus PK and efficacy studies.

Competing interests: P.A., T.W., E.D., C.S., R.P., E.K., R.H., C.M.T., J.K., F.C., I.P., L.T., C.R., Z.H.T., Ja.Wa., D.G., Jo. Wa. and I.R.C. were or are GSK employees; J.S. and R.V. are employees of OctoPlus N.V., a subsidiary of Dr. Reddy's Laboratories Ltd., P.M. & T.M.N. (OSOD) and J.P., T.S., S.S., C.S., and B.C. (Covance).

Conflict of interest statement: The authors have declared that no conflict of interest exists.

Appendix A. Supplementary data: Supplementary data to this article can be found online at <http://dx.doi.org/10.1016/j.jconrel.2016.10.026>.

co-polymer. The molecule was evaluated both *in vitro* for potency against VEGF and in ocular VEGF-driven efficacy models *in vivo*. The dual dAb is highly potent, showing a lower IC₅₀ than aflibercept in VEGF receptor binding assays (RBAs) and retaining activity upon release from microparticles over 12 months *in vitro*. Microparticles released functional dual dAb in rabbit and primate eyes over 6 months at sufficient levels to protect Cynomolgus against laser-induced grade IV choroidal neovascularisation (CNV). This demonstrates proof of concept for delivery of an *anti*-VEGF molecule within a sustained-release system, showing protection in a pre-clinical primate model of wet AMD over 6 months. Polymer breakdown and movement of microparticles in the eye may limit development of particle-based approaches for sustained release after IVT injection.

Keywords

VEGF; Choroidal neovascularisation; Sustained-release delivery; Intraocular injection; Microspheres; Non-human primate eyes

1. Introduction

Neovascular AMD is the most common cause of legal blindness in industrialised countries [1,2]. Pharmacotherapy by IVT administration of VEGF inhibitors has greatly improved patient outcomes [1,2,3], but the need for continuous therapy requiring frequent clinical visits for an increasing elderly population has become an issue [3]. Researchers and clinicians have been trying to extend IVT administration beyond monthly (ranibizumab) or bimonthly (aflibercept) labels [1]. The generation and validation of a controlled release system for wet AMD, with efficacy equivalent to standard of care (SoC), but enabling IVT administration once every six months is a significant goal [4]. Ocular implants for release of small molecule anti-inflammatory agents are already approved [5,6], and some surgical device implants are under evaluation in Phase I/II wet AMD trials for extended delivery of VEGF inhibitors [7,8]. The Forsight Vision 4/Genentech evaluation of a refillable device which is aiming to be topped up with ranibizumab every four months using a special loading needle is recruiting for a Phase II study [7]. Neurotech have performed both Phase I and II clinical trials with their intravitreally implanted encapsidated cell therapy device, (ECT), containing a cell line secreting a highly potent VEGF inhibitor, although the procedure appears well-tolerated, the Phase II trial was recently halted due to lack of reproducible long term efficacy [8]. However, no ocular controlled release system, administered by a simple IVT injection *via* a 30 g needle, enabling long-term biologic exposure has progressed beyond pre-clinical studies, [9]. A recent review emphasizes significant hurdles for integrating biologics within delivery matrices without disrupting their molecular integrity and activity. Controlling release rate to achieve therapeutic levels of biologics for more than a few months has been challenging [9].

In this paper, we address many of these challenges and describe a slow-release system with a potent *anti*-VEGF biologic [10]. The domain antibody based, dual dAb molecule [10,11] and a compatible delivery system were co-evaluated with the aim to generate a product for wet AMD, delivering 6 month protection after a single IVT injection. The delivery system is

based on PolyActive™, polyethylene glycol–polybutylphthalate (PEG-PBT) hydrogel *co*-polymer micro-particles [12,13]. The system and released molecule were evaluated *in vitro* for functionality and potency and *in vivo* in VEGF-driven ocular efficacy models.

2. Materials and methods

2.1. Study design

Objective was to show VEGF dual dAb (Fig. 1A), could load PolyActive microparticles in sufficient amounts to allow release of functionally active molecule *in vitro* and in vitreous over 6 months at levels capable of protecting in a Cynomolgus model of wet AMD. Achievement was demonstrated by physical and functional molecular assays *in vitro*, with *in vivo* experiments in rabbit and Cynomolgus. Assays used duplicate or triplicate samples: for immuno-assays IDBSXLFit with sigmoidal dose response using 4PL curves were used to generate EC₅₀ or IC₅₀ values and for PK analyses, noncompartmental PK with WinNonlin™ (WNL) v6.3 and tissue values were calculated assuming an extract density of 1 g/ml, i.e. $\text{tissue conc (ng/g)} = \text{extract conc (ng/ml)} \times \text{extract weight} / \text{tissue weight (g)}$. Animal studies were non-blinded, randomised pre-screened to exclude ocular abnormalities, pre-existing ADA responses or elevated baselines to immunoassays for ADA analyses positive cut-off points and outliers were determined based upon baseline measures (background + 1.645 × SD or mean signal for all tested samples + 3.09 × STDEV and ADA positives were excluded from PK and efficacy analyses. Group sample size for rabbit and Cynomolgus PK studies were chosen using variance in past experiments, for the laser CNV study a minimum sample size $n = 6$ was determined from previous analyses, (Covance database). Animal welfare (NIH) and reporting (ARRIVE, EQUATOR) guidelines were followed.

2.2. Generation and purification of domain antibody-based proteins

This was performed using phage-display isolation and standard technologies, for details see Supplementary data: materials and methods.

2.3. Particle sizing, light and scanning electron microscopy and protein release measurements

These were performed using standard methodology, for details see Supplementary data: materials and methods.

2.4. Functional, molecular integrity and receptor binding assays

These assays utilised mesoscale discovery platform (MSD) technology performed according to manufacturer's recommendations (MSD), for details see Supplementary data: materials and methods.

2.5. Cynomolgus PK and efficacy studies and pharmacokinetic modelling

Long term PK and efficacy studies are shown schematically in Figs. 3A and 4A, respectively and the extension of the efficacy study in Fig. S6A. Empty microparticles were prepared from the same polymer as 72F, as a negative control: Group 1, (Fig. S1A). IVT injections were performed on anesthetized animals and are described in detail in Supplementary data:

materials & methods, post-injection management included infection, pain and inflammation control. For details of the formulation administration, laser CNV, FA and extended PK studies and the pharmacokinetic modelling using WinNon lin™ and MATLAB see Supplementary data: materials & methods.

2.6. Statistics

For analysis of CNV lesion data, Fisher's exact tests in the R statistical environment compared the treatment groups based on a contingency table at each time point, [14,15], together with Poisson regression analysis, [16], to model count data at each time point with Dunnett's adjusted *P*-values in SAS using PROC GENMOD with JMP software used for data visualisation. Animals I00079, I00084, and I00085 were excluded from all analyses due to impact of ADA, (Table S6). Modelling simulations used a 2-compartment model (vitreous and serum) relying on compartment volumes and elimination rates determined from naked dual dAb ocular and systemic PK studies. For loaded microparticle studies, the model was extended to include a drug depot parameter: 'releasing into the vitreous' - release rate being defined by *in vitro* release data and adjusted with *in vivo* release data. SoC *anti*-VEGFs were simulated using a 1-compartment model and clearance rates from published data, details with codes and algorithms are shown in Supplementary data: materials and methods.

2.7. Study approval

All animal studies were reviewed and approved by the appropriate ethical review boards for animal experimentation under the existing licences. Rabbit studies, (GSK, UK) and non-human primate studies, (Covance, USA).

3. Results

3.1. Domain antibody molecules to VEGF

Different molecular formats are depicted in Fig. 1A, dual dAb; dAb-Fc and Fc-dAb: dual dAb, without C-terminal V κ dAbs or N-terminal V H dAbs, respectively. All molecules are homodimers linked by cysteine bridges, based upon human immunoglobulin G1 subclass Fc domain (IgG1Fc).

3.2. Generation and analysis of dual dAb-loaded PolyActive microparticles

Liquid concentrated dual dAb was incorporated into six PolyActive microparticle formulations with mean particle diameters of 62–66 μ m, encapsulation-efficiencies of 72% and protein loading of 15.3%, weight by weight, (w/w) using the water-in-oil-in-water emulsion (w/o/w) process, (Table 1, Fig. 1B, C, D, Fig. S1). The aim was to test variant formulations across three parameters: PEG length, PEG:PBT ratio and water/polymer (w/p) ratio, for dual dAb-release rate. *In vitro* release profiles show a small burst after 1 day (<20%), a potential loading dose suitable for immediate VEGF blockade; a predicted release period of: 6 months for formulations 72B and 72E, ('*fast*'); 9–12 months for 72F, ('*intermediate*') and 12–18 months for 72A, 72C and 72D, ('*slow*'), (Fig. 2A, Fig. S2A). *In vitro* release was monitored from all formulations for 6 months and extended to 12 months for 72F. Post-experiment dual dAb mass balances ('retained' plus 'released') of 79–95% were confirmed, with 84% release of dual dAb from 72F achieved by month 12, (Table 1).

3.3. Functional activity of dual dAb released from microparticle *in vitro*

Functional activity of released dual dAb in VEGF binding immunoassays was retained at >90%, over 6 months in all formulations except for 72A and 72D (70–90%), (Fig. 2B). Some partial dual dAb cleavage occurred at days 21–182, but after 6 months, molecular integrity was >50% after release from formulations 72B, 72E and 72F. Dual dAb functional activity was retained at >85% after 6–12 months release from 72F and protein integrity was 50% at 10 months (40% after 12 months). Functional activity for released, (72B, 72E and 72F) dual dAb was retained best in the VEGF R2 RBA, whereas 72D (*'slow'*) activity decreased with time, (Fig. S2B, S2C and Table S1). Partial cleavage at linker regions could be identified from the *in vitro* release samples, generating N-terminal Vh dAb-Fc or C-terminal Vk Fc-dAb molecule (Fig. 1A), both of which maintain *anti*-VEGF activity, Fc-dAb with similar potency to dual dAb and aflibercept. After 5–6 months, dual dAb released from 72B, 72E and 72F had IC₅₀ values close to naked molecule and aflibercept in the VEGF R2 RBA, (Fig. 2C).

3.4. Ocular PK from dual dAb-loaded microparticles in rabbit

Ocular pharmacokinetic (PK) experiments were performed with both naked dual dAb (Fig. S3A) and dual dAb loaded microparticles in rabbit, (Fig. S3B). Anti-drug antibody (ADA) responses were noted in serum and ocular samples. Ocular half-life of naked dual dAb, in ADA free animals, was 4.3 days, (Fig. S3A). An ocular PK study was undertaken in rabbit to compare the *in vitro* release rate of dual dAb to that *in vivo*, after IVT injection of three formulations: 72A (*fast*), 72B (*slow*) and 72F (*intermediate*). At 6 months, ADA-free rabbits dosed with 72F maintained significant vitreal levels of dual dAb (1 µg/ml) whereas those dosed with 72B maintained about 10-fold lower levels. Rabbits dosed with 72A had reduced levels and the most frequent ADA responses. VEGF immunoassays showed that *in vivo* released dual dAb was functionally active, (Fig. S3B). Given the ADA responses to dual dAb in rabbit, further studies were undertaken in primates to reduce the impact of immunogenicity.

3.5. Ocular PK from dual dAb-loaded microparticles in primates

An ocular and systemic (intravenous) PK assessment of naked dual dAb in Cynomolgus determined both vitreous and serum (from ocular and systemically administered), dual dAb half-lives, to be 3–3.5 days (without ADA), (Table S2, Fig. S4A & S4B). A longer ocular PK study in Cynomolgus after IVT injection of formulations: 72B, 72E and 72F was performed to assess ocular tolerance and immunogenicity of the dual dAb formulations. The aim was to confirm PK data from the rabbit microparticle study (Fig. S3B), utilising formulations retaining dual dAb functionality and integrity *in vitro* for the longest time (Fig. 2B, C). The study was performed in two phases, (Fig. 3A, Table S3), data summarising intravitreal dual dAb levels released from the 3 formulations over 6 months are shown in Table 2 and are from one eye in a single animal (Phase I), or a mean of OS (left) and OD (right) eyes from the same animal for each time point (Phase II). 72F maintained the highest concentrations of dual dAb on day 169 (Table 2), at 4–5 µg/ml. Serum PK data from the 2 Phase II animals dosed with 72F are shown in Fig. 3B, together with modelled vitreous time courses based upon simulated *in vitro* and serum release profiles for 72F in Cynomolgus in

Fig. 3C (Fig. S5 and Table S3). 72F maintains significant dual dAb levels over 6 months in the primate eye (Table 2); ADA analysis (Table S4) confirmed little impact on this experiment.

3.6. Ocular efficacy from dual dAb-loaded microparticles in Cynomolgus

An ocular efficacy, laser CNV experiment was performed in Cynomolgus after IVT injection of 72F with the aim to demonstrate protection in this model [17]. A schematic design is shown in Fig. 4A. The non-human primate (NHP) laser CNV model typically has an incidence of 20–60% of laser spots developing Grade IV lesions by 2–3 weeks post-laser [18].

The aim was to determine whether a single administration of dual dAb would prevent CNV when administered in 72F (Group 2), over 3–4 or 5–6 months. Additionally, 2 different doses of naked molecule (Group 3), which matched modelled ‘burst’ and ‘trough’ release levels of dual dAb, (Fig. 4A), from 72F in the cyno PK study, (Table 2, Fig. 3C), were also analysed for protection in the laser-induced model of wet AMD. Eylea® (aflibercept) at 2 mg/eye (clinical dose) was used as both negative and positive control, dependent upon administration timing ahead of laser exposure, (Group 4). Naked aflibercept at human clinical doses was chosen for this control as it is predicted to become the SoC for treatment of wet AMD, [1].

Selection of eyes for each laser event is detailed in Table S5. Individual animal grade IV laser CNV lesion scores are shown in Table S6; a summary of the results, including statistical analysis, are shown in Table 3, where only separate eyes from ADA-free animals are considered. Example retinal fluorescence angiograms, (FA), from animals dosed with empty and dual dAb-loaded microparticles and aflibercept, (positive control), are shown in Fig. 4B.

Serum PK and ADA to dual dAb were monitored throughout, (Fig. S6), and ocular PK and ADA analysis were taken from animals selected post-laser for euthanasia, (Table S7, S8). In ADA free animals, intact serum dual dAb was detectable at 9 months. The Vh/Vk assay measures molecular integrity whereas the VEGF assay shows functional activity, even with partial molecule breakdown. A comparative analysis between the two assays suggests that molecular breakdown *in vivo* was not a major contributor to differences in dual dAb sera levels from these assays over time (Fig. S6C).

IVT injection with aflibercept was both a positive control (OS) and a comparator article (OD) in this study. Injection (OS) at day 141 and laser at day 148, led to complete inhibition of Grade IV CNV formation (0%), days 14 and 21 post-injection (Table 3, S6 and Fig. 4B and C). No inhibition of Grade IV CNV occurred post-laser, days 14 (38.9%) and 21 (31.5%) when laser treatment was 3–4 months post aflibercept dose, (OD), this is consistent both with the known half-life of aflibercept leading to clearance and no protection and an expected laser lesion frequency from historical data of negative control animals (19).

Inhibition of Grade IV CNV by dual dAb-loaded 72F was impacted by ADA development. ADA responses appeared at week 9 post-dose in sera of 5 animals given 72F (Table S8), and

continued through induction of lesions. ADA-positive eyes were removed from data analysis, (Table S6, Fig. S6) and 72F treated ADA-negative eyes (Table 3) had an incidence of Grade IV laser CNV of 7.4–9.3% (day 92) and 4.4–11.1% (day 148). Of the 5 ADA-negative eyes after day 148 laser, in 4, Grade IV CNV was completely absent, (0/9). The study was powered to detect a near complete inhibition of Grade IV CNV lesions, ($n = 6$). Original 72F-dosed animals, ($n = 10$) were reduced ($n = 5$), by early euthanasia or ADA presence. As this was only one animal less than anticipated, a comparative statistical analysis was performed using both the Fisher's exact test and Poisson regression, (Dunnett's test). Differences between 72F and empty microparticle dosed animals lasered at day 92 were not statistically significant, perhaps because lesion formation in the negative control group was at the low range of what is normally observed (Table 3), [20], Differences between 72F and aflibercept dosed animals (OD) at day 92 when aflibercept levels were exhausted were statistically significant (Table 3, Table S9). At the day 148 laser, both tests supported a statistical difference, 5–6 months post-dose, between levels of Grade IV CNV in 72F dosed ADA-negative, compared to empty microparticle dosed animals, (Table 3, Table S9), [14,15,16,20], indicating that dual dAb release at 6 months was sufficient to ameliorate Grade IV lesion development. A graphical comparison of the range of Grade IV lesion responses across the groups after the 2nd laser (Table 3, S6) is shown in Fig. 4C, demonstrating the statistical difference ($***P < 0.001$, Fisher's exact test) when only ADA negative animals (circles) are considered. Further analyses performed on the laser CNV findings within treatment groups included grade II and III lesion assessment as these have increased hypofluorescence and leakage in fluorescein angiography (FA), Fig. 4D [21]. Data confirmed dual dAb levels released at 6 months from 72F resulted in significant reductions in CNV lesion pathology and median lesion grade compared to empty microparticle dosed animals. In support of this conclusion, naked dual dAb at the predicted 'trough' 16 μg (1.9%) and 'burst' 160 μg (0%) per eye doses, expected to be released by 72F, were effective at preventing Grade IV CNV lesions at 14/21 days post-dose/post-laser (Table 3, Fig. 4).

3.7. Adverse events in long term ocular PK and efficacy studies in Cynomolgus

Adverse and unexpected events occurred in both ocular microparticle studies in Cynomolgus: particle migration from vitreous to anterior chamber, (Fig. 5A), delayed polymer breakdown, (Fig. 5B) and ocular inflammation, (Fig. 5C).

Microparticles first appeared in the anterior chamber at day 3 after IVT injection, moving through the vitreous and migrating into the anterior chamber, (Fig. 5A). The frequency and volume of migration increased with time, peaking at day 60 and occurring for both empty and dual dAb-loaded microparticles, (Tables S10A, S10B). In the PK study, migration occurred in 11/18 eyes (61%) and for the efficacy study in 13/32 eyes (41%): an average of 48%. Fig. 5A shows an example where microparticles are seen as a white crescent, (OS, anterior chamber), day 16, the total amount increasing at day 64. The similarly dosed OD from the same animal shows no particle migration. Isolation of 72F microparticles from aqueous humour at 6 months and size determination by light microscopy were similar to those originally dosed into vitreous. The exact mechanism of movement remains unresolved.

Of concern were observations that ocular 72F polymer breakdown rate was slower than molecule release rate. Microparticle degradation rate was not quantified; small numbers of Cynomolgus eyes were imaged 6–12 months post dose, (Fig. 5B) and show that polymer material in the vitreous reduces from 6 to 12 months but there is not full degradation. By 12 months, *in vitro* release of dual dAb from 72F was 84% complete (Table 1). In similar rabbit studies, 72F microparticle pellets were recovered from vitreous after six months and were partially degraded.

Acute transient inflammation occurred in Cynomolgus after IVT administration of all microparticle formulations in both PK and efficacy studies (Table S11). Ocular histopathology was performed after euthanasia for selected animals from the efficacy study, to review inflammatory and morphological effects (Table S12). Fig. 5C shows examples of such effects: microparticles in ventral filtration angle and organizing connective tissue (I00072) and anterior segment inflammation (I00085). Microparticles and macrophage/multinucleate giant cell inflammation correlated with ophthalmic examination findings of vitreous haze and/or vitreous cells. Perivascular sheathing was seen in some animals in both studies and was linked to ocular ADA and blood retinal barrier (BRB) breakdown enabling entry of systemic ADA in to the vitreous (Table S4, S8). Veterinary intervention was required in some microparticle-dosed animals to control sporadic ocular inflammation. Two animals dosed with dual dAb-loaded microparticles showed ocular inflammation, driven by severe persistent ADA leading to early euthanasia; although some animals dosed with 72F were monitored for 9–12 months without major issues.

4. Discussion

Cynomolgus studies demonstrated ocular PK and efficacy over 6 months following a single IVT administration of 72F. The effect on Grade IV CNV lesions is important because these closely resemble active classical CNV lesions seen in human AMD [17]. Three further hurdles would need to be addressed to translate this and potentially other particulate IVT injectable controlled release systems delivering biologic VEGF inhibitors in to a drug product for clinical use:-

- i. particle migration from vitreous to anterior chamber
- ii. delayed polymer breakdown compared to payload release
- iii. ocular inflammation (both acute initial and later stage *anti*-molecule immunogenicity).

Although all three issues were highlighted for both empty and dual dAb-loaded microparticles in the Cynomolgus studies described in this work, there are further complications of later stage inflammatory responses that could additionally be contributed to by ADA/immunogenicity in pre-clinical species that may only be fully relevant to loaded microparticles.

One explanation for particle migration is movement mediated by accommodation mechanisms in young primates, driven by ciliary muscle changes upon disaccommodation, leading to fluid flow and microparticle migrations from vitreous to anterior chamber

[22,23,24]. No migration was observed in multiple IVT-injected microparticle rabbit studies, but rabbits have different accommodation mechanisms compared to NHPs and humans [25]. Researchers developing particulate systems for IVT injection have not previously reported this finding, however, triamcinolone in the rhesus monkey [22] and other particles have been seen to move from vitreous to anterior chamber [26], Mary Ann Croft, personal communication]. This was described with Indian Ink particles in the early 20th century [27] and some clinical cases present a pseudohypopyon after IVT injection, consisting of triamcinolone crystals in the anterior chamber [28]. Although many elderly patients with wet AMD may lose full accommodative function, this can deteriorate both in aged NHPs and at >50 years in man [29,30]. Further work in primates would need to mitigate these concerns prior to the clinic. It may be difficult for long term particulate delivery systems to progress *via* IVT injection in man [31]. Replacing particulates with solidifying erodible injectable gels may circumvent some of these issues [32,33].

PolyActive polymers as implants or delivery systems have been studied extensively in pre-clinical models, also in the clinic in the subcutaneous setting [12,13,4,34–37], but degradation rate and compatibility within the eye have not been previously studied. Historical work suggested a potential 9 month breakdown time *in vivo*, a 6–9 month breakdown time would most likely be acceptable for the release kinetics demonstrated in these studies. Studies in the rabbit eye did not predict the large mass of microparticles visualised 10–12 months post IVT injection in Cynomolgus, (Fig. 5B). *In vitro* release studies did suggest microparticles could remain intact for 12 months but degradation was expected to be accelerated *in vivo* [12,13,34–37]. Also the rabbit studies also did not demonstrate the particle migration, the combination of the two phenomenon in Cynomolgus and likely man would limit re-dosing of formulations that showed both migration and slow-degradation.

Acute initial ocular inflammation may have been avoided using formulations prepared using good manufacturing practice (GMP) with highest purity raw materials, but in current studies, microparticles were prepared aseptically and contaminants and leachables such as endotoxin and dichloromethane (DCM) were below acceptable limits. Note that in the rabbit studies described in this work, (Fig. S3), and other rabbit studies with PolyActive microparticles from these batches, initial ocular inflammation was not as acute as in the Cynomolgus. Surface hydrophobicity can contribute to nanoparticle biocompatibility issues in lung [38]. PolyActive microparticles are amphiphilic consisting of hydrophilic (PEG) and hydrophobic (PBT) components, with PEG being close to the surface. It seems unlikely hydrophobicity is a major contributor to rapid transient inflammation which was similar across all PolyActive formulations dosed in the PK study, although 72B and 72E are less hydrophobic than 72F. An increase in microparticle hydrophobicity with time as PEG dissociates, could contribute to later inflammation in the two Cynomolgus studies, but *anti*-molecule ADA links to later and more severe inflammatory responses and could be solely responsible.

Ocular inflammatory damage from ADA responses to dual dAb may primarily be a reaction to humanised protein in Cynomolgus. The molecule is clearly highly immunogenic in rabbit. The specificity of the ADA was further characterised in both rabbit and Cynomolgus (ten samples), and the majority of the response was to the complementarity determining regions,

(CDRs) binding to VEGF, within the intact dual dAb molecule and largely to the CDRs within the Vh dAbs. In some cases in Cynomolgus, impact was severe and would be concerning if directly translated to man. However, other biologics that have high immunogenicity in pre-clinical species have been licensed and are marketed drugs in man: one example is the anti Tumour Necrosis Factor (TNF) monoclonal antibody adalimumab (Humira), [39], although early ranibizumab (Lucentis), formulations were also inflammatory in preclinical species [40]. Dual dAb has been screened for pre-existing immunogenicity using sera from a small panel of human donors and ADA responses were not detected. Development of post-dose ADAs would need to be explored in man for a multiple administration regime. Ocular reaction to microparticles and any migration would need careful control in the human setting.

Key factors enabling the successes described in this study are the co-evolution of a delivery system and potent molecule, highly stable over time, compatible with aqueous, hydrogel formulation, with effective function even after reductions in molecular integrity. Dual dAb degradation after release *in vitro* was partial up to 365 days and explicable by combinations of metal ion induced immunoglobulin hinge and protease linker cleavage. Similar degradation paths could be seen in accelerated breakdown studies of naked molecule so there does not appear to be significant particle-induced degradation of the molecule, in contrast to the behaviour of poly lactic-*co*-glycolic acid, (PLGA) microparticles [41]. PolyActive hydrogel formulation 72F retained dual dAb functional activity over 6–12 months both *in vitro* and *in vivo* and controlled a size-dependent release rate over time. Other key features are the ability to concentrate the molecule to >200 mg/ml as a solution, a high percentage protein loading to microparticles (22% w/w) and a simple injection enabling maximum theoretical particle dose (up to 7.5 mg or 15%) in a 50 μ l volume *via* a 30 g needle and 0.5 ml syringe.

5. Conclusions

A single 72F injection is efficacious in the cynomolgus laser CNV model at 6 months, but translating efficacy to man requires mathematical modelling. Multiple lines of evidence, including *in vitro* potency, dual dAb enhanced stoichiometry [10], comparable size and ocular PK [19] and similar vitreal concentrations of naked dual dAb compared to aflibercept at the time of protection in ocular efficacy models (*ca.* 8 μ g/ml, Fig. 6A, [42]) demonstrate that dual dAb is at least equipotent to aflibercept *in vivo*. Maintenance of dual dAb vitreous levels similar or greater than aflibercept therefore should predict efficacy in wet AMD patients.

An initial step converting Cynomolgus ocular PK to human is in understanding how *in vivo* release of dual dAb from 72F differs from that *in vitro*. Simulations of Cynomologus vitreous and serum PK were obtained using a two compartmental model of vitreous and serum, and the *in vitro* release data, (Fig. 6B: red traces) and were found to be significantly different to observed PK data (Fig. 6B: blue and purple traces). These simulations show that *in vivo* release is faster than *in vitro* over the first few months and that microparticles become exhausted of dual dAb faster *in vivo*, leading to slower release beyond 6 to 7 months. This finding is not unexpected as many polymers do not show a directly comparable

release rate for proteins both *in vitro* and *in vivo*, although PolyActive shows quite a close relationship [12,13]. A faster ‘burst’ release *in vivo* compared to *in vitro* could be related to the more dilute concentration *in vivo*, or to the initial acute inflammatory response seen in Cynomolgus. The most likely first step is the initial release of surface bound PEG from the microparticles and this may have been faster *in vivo* than *in vitro* and perhaps led to increased protein release.

Human vitreal dual dAb PK was simulated (Fig. 6C, blue line) by adjusting the vitreal volume and half-life in the Cynomolgus two compartmental model based upon the larger human eye. Dual dAb vitreal release was simulated using an estimated human dose, which had already been achieved in the Cynomolgus studies (7.5 mg microparticles, 22% loading of 1.7 mg dual dAb) in 50 μ l injection volume and the *in vivo* release rate previously fit to the Cynomolgus efficacy PK data for 72F. For comparison, SoC (ranibizumab and aflibercept) PK was simulated, (Fig. 6C, green and red lines, respectively), using known or estimated vitreous clearances; both fall to similar trough levels (*ca.* 7 μ g/ml) in line with their market labels at 1 and 2 months respectively. Initial concentrations of released dual dAb are lower than ranibizumab or aflibercept, simulated human vitreous levels of dual dAb still exceed SoC at 6 months indicating real potential for an effective 6-monthly dosing regime.

If the other challenges highlighted in the discussion can be resolved, single administration of an *anti*-VEGF biologic formulation could be possible to increase patient/provider compliance and relieve patient burden in wet AMD.

Supplementary Material

Refer to Web version on PubMed Central for supplementary material.

Acknowledgments

Funding: GSK funded the work.

Authors dedicate the work to the late Prof Henry F. (Hank) Edelhauser, Emory Eye Center, Georgia, USA. We thank *anti*-VEGF SR programme teams (UK & USA) and ex-GSK Ophthalmology: D. Lee, M. McLaughlin, F. Lopez and C. Bruck. Thanks due to P. Topley, GSK Laboratory Animal Support for rabbit studies: G. Whelan (veterinary), P. Clements and C. Newman (analysis). Thanks for help with dual dAb production, formulation and biophysics: to G. Finka, P. Steward, G. Oladiran, R. Shah, C. Qvist, R. Caimi and A. Ketkar. Light microscopy and scanning electron microscopy (SEM) at GSK: R. McKeown, T. Boran and N. Mistry. Statistical help: A. Wan; human pre-existing immunogenicity assessment: M. Birchler. V. Damian-Iordache for ocular modelling capabilities. C. Routledge and H. Cowley for translational medicine; L. Jespers, G. Gough, A. Basran and S. Khan for project support; G. Moolhuizen and J. Van der Zwan at OctoPlus (Dr. Reddys) and Covance study monitors M. Hall and C. Trost; GSK counterparts: C. Overvold, J. Wilson and J. Speitel. Help with Figures: M. Gallucci. T. Michael Nork is supported by *Research to Prevent Blindness*.

References

1. Freund K, Mrejen S, Gallego-Pinazo R. An update on the pharmacotherapy of neovascular age-related macular degeneration. *Expert Opin Pharmacother.* 2013; 14:1017–1028. [PubMed: 23560774]
2. Cheung N, Lam D, Wong T. Anti-vascular endothelial growth factor treatment for eye diseases. *Br Med J.* 2012; 344:e2970. [PubMed: 22549056]

3. Schmidt-Erfurth U, Chong V, Loewenstein A, Larsen M, Souied E, Schlingemann R, Eldem B, Mones J, Gisbert R, Bandello F. Guidelines for the management of neovascular age-related macular degeneration by the European Society of Retina Specialists (EURETINA). *Br J Ophthalmol*. 2014; 98:1144–1167. [PubMed: 25136079]
4. Barman SP. Ocular drug delivery: review of present technologies and steps forward. *ONdrugDELIVERY*. 2014; 48:4–7.
5. Kuno N, Fujii S. Recent advances in ocular delivery systems. *Polymer*. 2011; 3:193–221.
6. Cunha-Vaz J, Ashton P, Iezzi R, Campochiaro P, Dugel PU, Holz FG, Weber M, Danis RP, Kupperman BD, Bailey C, Billman K, Kapik B, Kane F, Green K. Sustained delivery fluocinolone acetonide vitreous implants: long term benefits in patients with chronic diabetic macular edema. *Ophthalmology*. 2014; 121:1892–1903. [PubMed: 24935282]
7. <http://www.mddionline.com/article/genentech-betting-device-approach-block-buster-12-10-15>.
8. <http://www.neurotechusa.com/VEGF-Antagonist.html>.
9. Kim Y, Chiang B, Wu X, Prausnitz M. Ocular delivery of macromolecules. *J Control Release*. 2014; 190:172–181. [PubMed: 24998941]
10. Walker A, Chung CW, Neu M, Burman M, Batuwangala T, Jones G, Tang CM, Steward M, Mullin M, Tournier N, Lewis A, Korczynska J, Chung V, Catchpole IR. Novel interaction mechanism of a domain antibody based inhibitor of human vascular endothelial growth factor with greater potency than ranibizumab and bevacizumab and improved capacity over aflibercept. *J Biol Chem*. 2016; 291:5500–5511. [PubMed: 26728464]
11. Enever C, Pupecka-Swider M, Sepp A. Stress selections on domain antibodies: ‘what doesn't kill you makes you stronger’. *Protein Eng Des Sel*. 2015; 28:59–66. [PubMed: 25655396]
12. Deschamps AA, Van Apeldoorn AA, Hayen H, De Bruijn JD, Karst U, Grijpma DW, Feijen J. *In vivo* and *in vitro* degradation of poly(ether-ester) block copolymers based on poly(ethylene glycol) and poly(butylene terephthalate). *Biomaterials*. 2004; 25:247–258. [PubMed: 14585712]
13. van Dijkhuizen-Radersma R, Hesseling SC, Kaim PK, de Groot K, Bezemer JM. Biocompatibility and degradation of poly(ether-ester) microparticles: in vitro and in vivo evaluation. *Biomaterials*. 2002; 23:4719–4729. [PubMed: 12361610]
14. Fisher RA. On the interpretation of χ^2 from contingency tables, and the calculation of P. *J R Stat Soc*. 1922; 85:87–94.
15. Fisher, RA. *Statistical Methods for Research Workers*. 11th. Oliver and Boyd; Edinburgh: 1954. eleventh edition
16. Cameron, AC., Trivedi, PK. *Regression Analysis of Count Data*. Camb Univ Press; Cambridge: 1998.
17. Krzystolik MG, Afshari MA, Adamis AP, Gaudreault J, Gragoudas EE, Michaud NA, Li W, Conolly E, O'Neill CA, Miller JW. Prevention of experimental choroidal neovascularization with intravitreal anti-vascular endothelial growth factor antibody fragment. *Arch Ophthalmol*. 2002; 120:338–348. [PubMed: 11879138]
18. Ryan SJ. Subretinal neovascularization. Natural history of an experimental model. *Arch Ophthalmol*. 1982; 100:1804–1809. [PubMed: 6182868]
19. Center for drug evaluation and research Pharmacol Rev. BLA 125387Orig1s000. 2012
20. Dunnett CW. A multiple comparison procedure for comparing several treatments with a control. *J Am Stat Assoc*. 1955; 50:1096–1121.
21. Lichtlen P, Lam TT, Nork TM, Streit T, Urech DM. Relative contribution of VEGF and TNF- α in the Cynomolgus laser-induced CNV model: comparing efficacy of bevacizumab, adalimumab and ESBA105. *IOVS*. 2010; 51:4738–4745.
22. Croft MA, Nork TM, McDonald JP, Katz A, Lutjen-Drecoll E, Kaufman PL. Accommodative movements of the vitreous membrane, choroid, and sclera in young and presbyopic human and nonhuman primate eyes. *IOVS*. 2013; 54:5049–5058.
23. Croft MA, McDonald JP, Katz A, Lutjen-Drecoll E, Kaufman PL. Extralenticular and lenticular aspects of accommodation and presbyopia in human versus monkey eyes. *IOVS*. 2013; 54:5035–5048.
24. Lutjen-Drecoll E, Kaufman PL, Wasielewski R, Li LT, Croft MA. Morphology and accommodative function of the vitreous zonule in human and monkey eyes. *IOVS*. 2010; 51:1554–1564.

25. Croft MA, Glasser A, Kaufman PL. Accommodation and presbyopia. *Int Ophthalmol Clin.* 2001; 41:33–46.
26. Croft MA, Nork TM, McDonald JP, Heatley GA, Katz A, Kaufman PL, Lutjen-Drecoll E. Mechanism of accommodation: new findings and the implications for presbyopia. *IOVS.* 2013; 56:3568.
27. Paterson JV. Some observations on the lymph flow through the eyeball in man and certain animals. *J Pathol Bacteriol.* 1904; 9:323–337.
28. Salz D, Prenner J, Emmett NJ, Cunningham T. Local complications of IV anti-VEGF therapy. *Rev Ophthalmol.* Nov 16.2010 10(2010)
29. Plainis, S., Chairman, WN., Pallikaris, IG. The Physiologic Mechanism of Accommodation, Cataract and Refractive Surgery Today Europe. Apr. 2014 <http://crstodayeurope.com/2014/04/online> April 2014
30. Croft MA, McDonald JP, Nadkarni NV, Lin TL, Kaufman PL. Age-related changes in centripetal lens movement in monkeys. *Exp Eye Res.* 2009; 89:824–832. [PubMed: 19635475]
31. Cardillo JA, Souza-Filho AA, Oliveira AG. Intravitreal Bioerudivel sustained-release triamcinolone microparticles system (RETAAC). Preliminary report of its potential usefulness for the treatment of diabetic macular edema. *Arch Soc Esp Ophthalmol.* 2006; 81:675–682. [PubMed: 17199160]
32. Mitragotri S, Burke PA, Langer R. Overcoming the challenges in administering biopharmaceuticals: formulation and delivery strategies. *Nat Rev Drug Discov.* 2014; 13:655–672. [PubMed: 25103255]
33. Yang JA, Yeom J, Hwang BW, Haffman AS, Hahn SK. *In situ*-forming injectable hydrogels for regenerative medicine. *Prog Polym Sci.* 2014; 39:1973–1986.
34. Bezemer JM, Radersma R, Grijpma DW, Dijkstra PJ, Feijen J, van Blitterswijk CA. Microparticles for protein delivery prepared from amphiphilic multiblock copolymers. 1. Influence of preparation techniques on particle characteristics and protein delivery. *J Control Release.* 2000; 67:249–260. [PubMed: 10825558]
35. Bakkum EA, Trimbos JB, Dalmeyer RAJ, van Blitterswijk CA. Preventing postoperative intraperitoneal adhesion formation with PolyActive, a degradable copolymer acting as a barrier. *J Mater Sci Mater Med.* 1995; 6:41–45.
36. Beumer GJ, van Blitterswijk CA, Ponc M. Biocompatibility of degradable matrix induced as a skin substitute: an *in vivo* evaluation. *J Biomed Mater Res.* 1994; 28:545–552. [PubMed: 8027095]
37. Beumer GJ, van Blitterswijk CA, Ponc M. Degradative behaviour of polymeric matrices in (sub) dermal and muscle tissue of the rat: a quantitative study. *Biomaterials.* 1994; 15:551–559. [PubMed: 7918908]
38. Jones MC, Jones SA, Riffo-Vasquez Y, Spina D, Hoffman E, Morgan A, Patel A, Page C, Forbes B, Dailey LA. Quantitative assessment of nanoparticle surface hydrophobicity and its influence on pulmonary biocompatibility. *J Control Release.* 2014; 183:94–104. [PubMed: 24657808]
39. <http://www.fda.gov/downloads/Drugs/DevelopmentApprovalProcess/HowDrugsareDevelopedandApproved/ApprovalApplications/TherapeuticBiologicApplications/ucm092772.pdf>.
40. http://www.ema.europa.eu/docs/en_GB/document_library/EPAR_-_Scientific_Discussion/human/000715/WC500043550.pdf.
41. Blanco D, Alonso MJ. Protein encapsulation and release from poly (lactide-coglycolide) microspheres: effect of the protein and polymer properties and of the co-encapsulation of surfactants. *Eur J Pharm Biopharm.* 1998; 45:285–294. [PubMed: 9653633]
42. Nork TM, Dublitzig RR, Christian BJ, Miller PE, Miller JM, Cao J, Zimmer EP, Wiegand SJ. Prevention of experimental choroidal neovascularisation and resolution of active lesions by VEGF trap in nonhuman primates. *Arch Ophthalmol.* 2011; 129:1042–1052. [PubMed: 21825187]

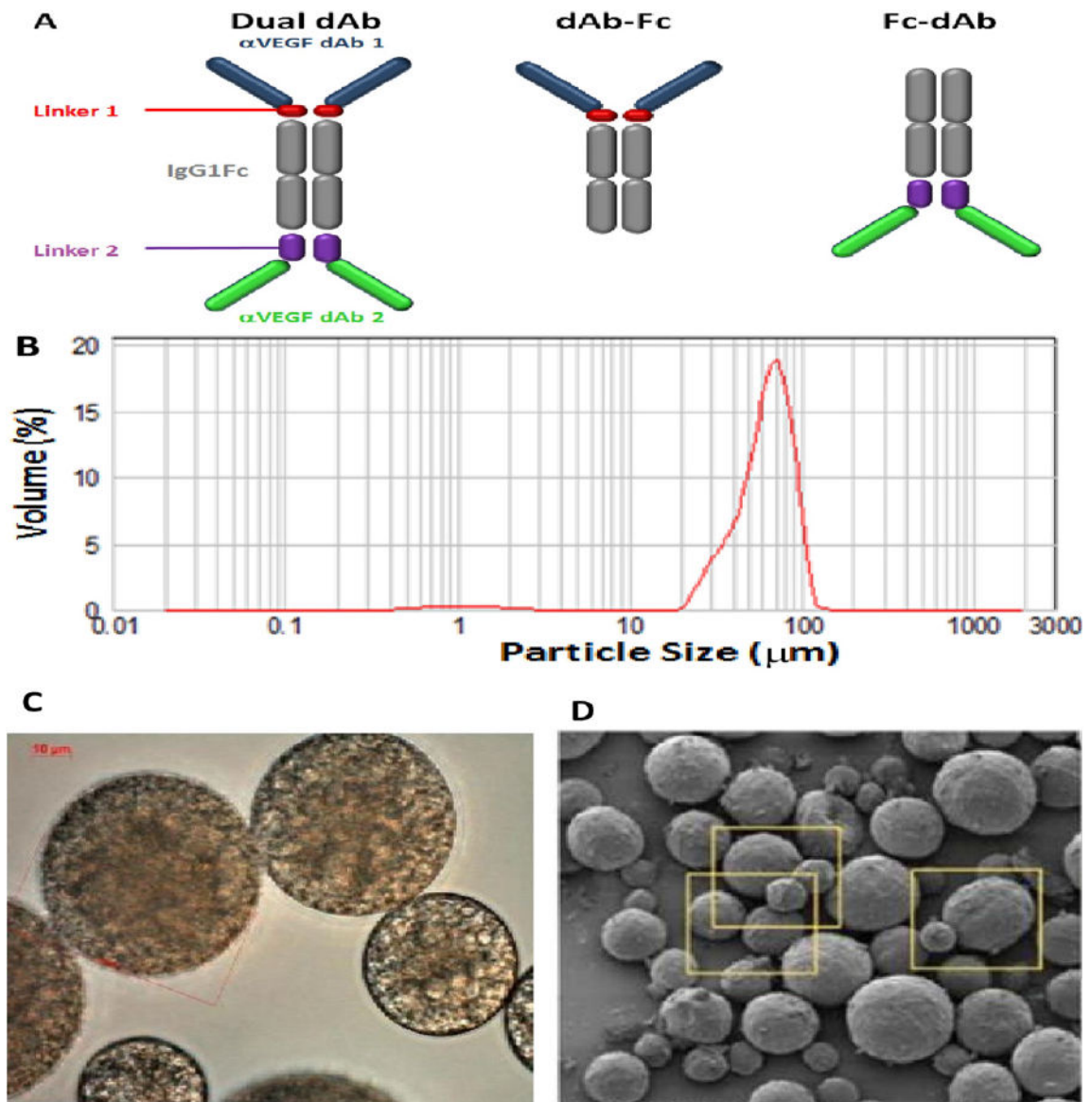


Fig. 1. (A) Schematic of *anti*-VEGF biologics: dual dAb, 109 kD, VEGF dAb-Fc, (top half, dual dAb), 79 kD, VEGF Fc-dAb, (bottom half, dual dAb), 79 kD. Characterisation of microparticle formulations: (B) Particle size analysis, 72F, (Table 1, Fig. S1A), (C) light microscopy analysis at high magnification, 1000 \times (D) Scanning Electron Microscopy (SEM) analysis at low magnification, 72F (yellow squares are displayed at 3 \times magnification in Fig. S1D).

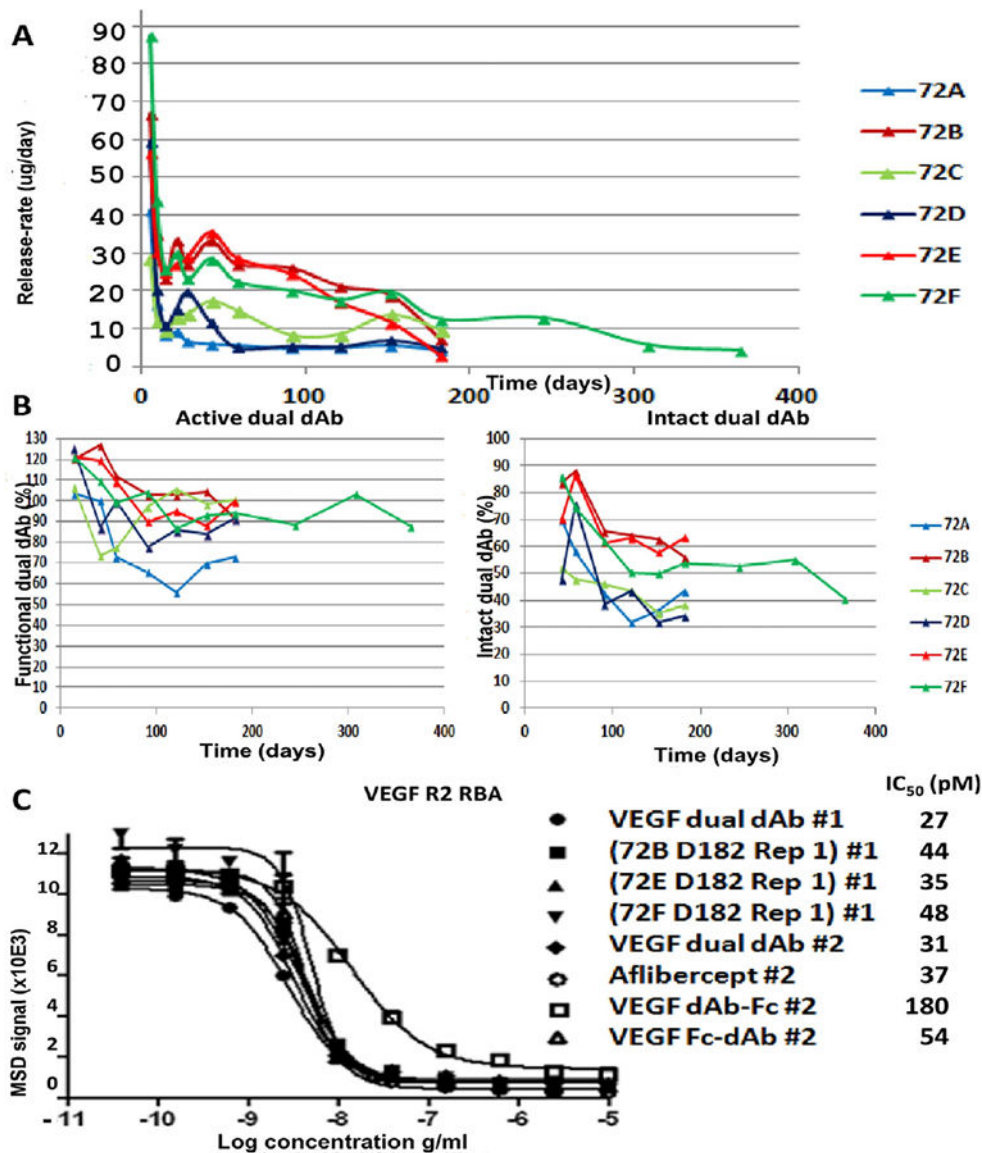


Fig. 2. (A) Release-rate/day for: 72A, 72B, 72C, 72D, 72E and 72F. All data is displayed without error bars for clarity of comparison, for release-rate/day, SD across triplicate samples at each time point for all formulations ranged from $\pm 0.2\%$ to $\pm 25\%$ of mean calculated values. Activity and integrity of dual dAb released from 72A-72F *in vitro*: (B) Percentage functional activity and intact molecule, for percentage functional activity/intact molecule scoring, SD across replicates, (2–3 samples) at each time point ranged from $\pm 0.7\%$ to $\pm 25\%$ of mean calculated percentage values (C) Functional activity of dual dAb released from 72B, 72E and 72F at D182 by inhibition of VEGF R2 RBA *cf.* dAb-Fc, Fc-dAb and aflibercept. Samples #1 and #2 were analysed on the same day on separate plates, (Fig. S2 and Table S1). SD error bars can be seen on some samples but variation is so low in other samples that these are within the region of the plotted symbol.

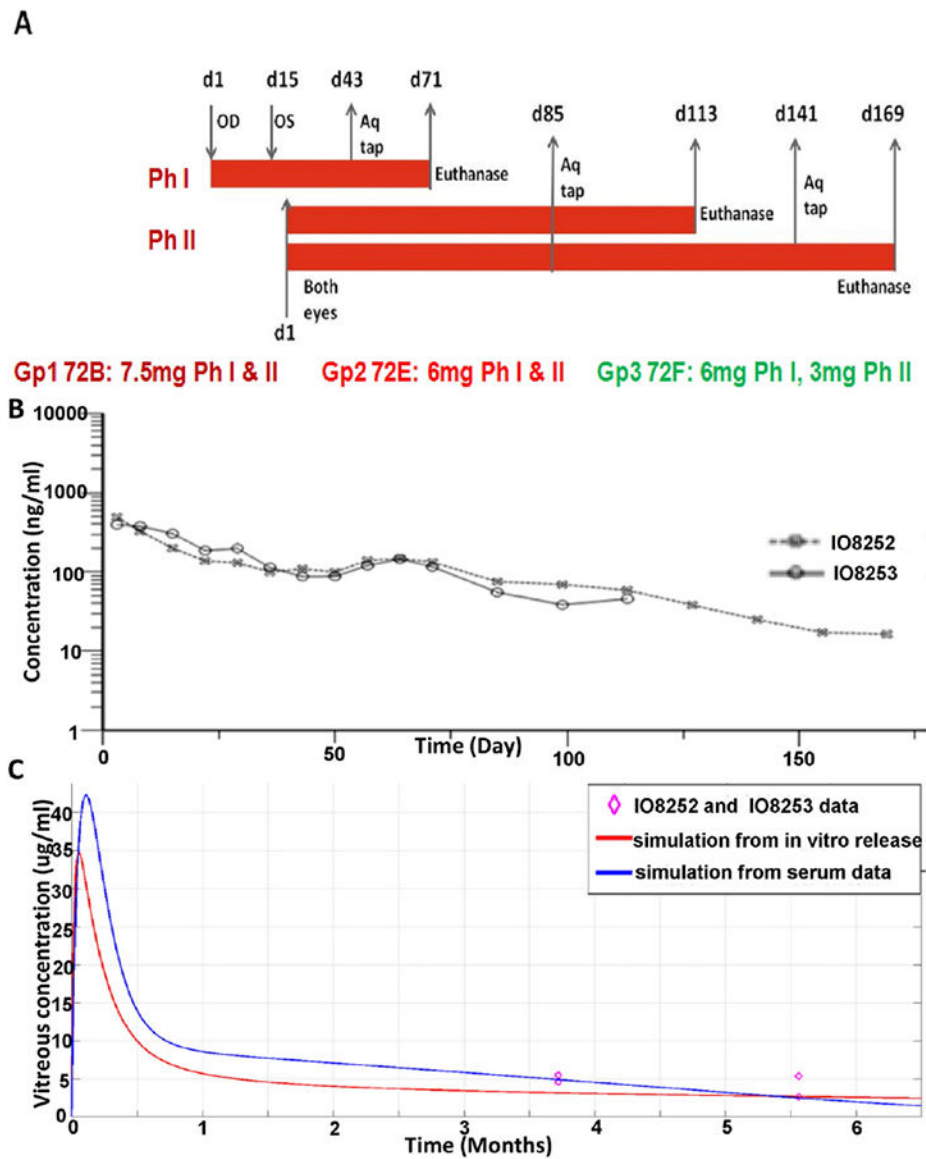


Fig. 3. PK from single IVT injection of dual dAb-loaded microparticles into Cynomolgus eye. OD = right eye, OS = left eye, (A) schematic PK experimental design, Gp = group, Ph = phase, Aq tap = aqueous humour sample, (B) serum concentration profiles from two 72F-dosed animals, (C) actual (VEGF MSD) and modelled, (*in vitro* released, red line, Fig. 1D; serum-released, blue line, Fig. S4D), vitreous dual dAb concentrations (Table 2, Table S3), purple () = data points (Table 2).

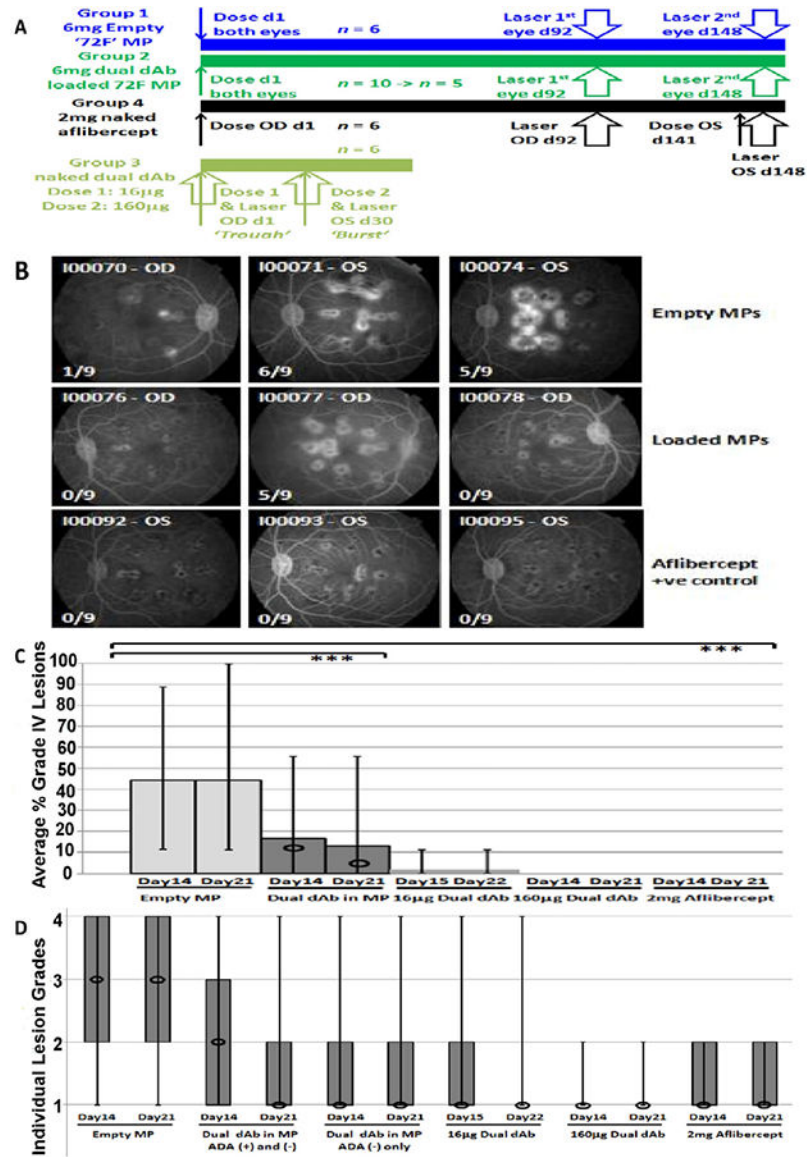


Fig. 4. Efficacy from single IVT injection of dual dAb-loaded microparticles into Cynomolgus eye. (A) Schematic efficacy experimental design, MP = microparticles. (B) Representative fluorescein angiograms (FA), 14 days after 2nd laser (Table 3) from empty (Group 1) and dual dAb-loaded (Group 2) microparticle dosed animals and positive control, aflibercept, (Group 4), dosed 1 week before laser. ×/9 = grade IV lesion score; (C) Box plot, average percentage grade IV lesions after 2nd laser for Groups 1, 2 and 4 and laser for Group 3 (naked dual dAb 2 doses): data across groups, columns = means, vertical lines = full response ranges, circles = means (ADA negative animals), ****P* < 0.001, (D) Box plot, individual lesion grades, after 2nd laser for Groups 1, 2, 4 and laser for Group 3, (naked dual dAb: 2 doses). Boxes show 25th to 75th percentiles, (box absence means both percentiles equal a lesion grade of 1), vertical lines = full response ranges, circles = median.

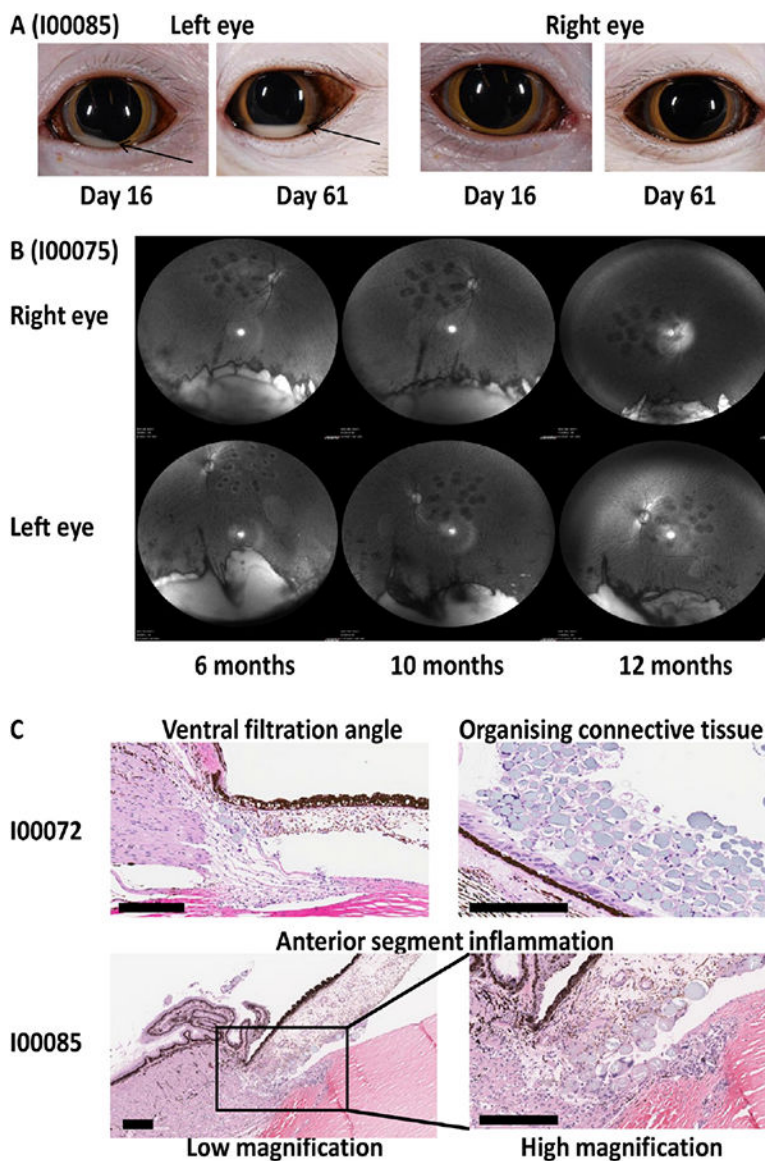


Fig. 5. Adverse events in Cynomolgus eye after IVT injection of microparticles. (A) Movement of microparticles from vitreous to anterior chamber. Images from both eyes of I00085 (Group 2: 72F) from efficacy study, at two different times. (B) Microparticle presence in Cynomolgus eye with time. Images taken from both eyes of I00075 (empty microparticles) using infra-red (IR) mode on Heidelberg Spectralis instrument with ultra-wide angled lens, from 6 to 12 months post-injection. Microparticles, reflecting light are in white area at the image base, temporal panels can be aligned using laser burn remnant. (C) Analysis by histopathology. Images taken from eyes of animals euthanized at day 170, after second laser, from efficacy study. Microparticles and multinucleated giant cells are highlighted in ventral filtration angle of animal I00072 (OS, Group1: empty microparticle-dosed) with organizing connective tissue in vitreous. Anterior segment inflammation is shown in animal I00085 (Group 2: 72F) at both low and high magnification. Scale bar, 200 μm .

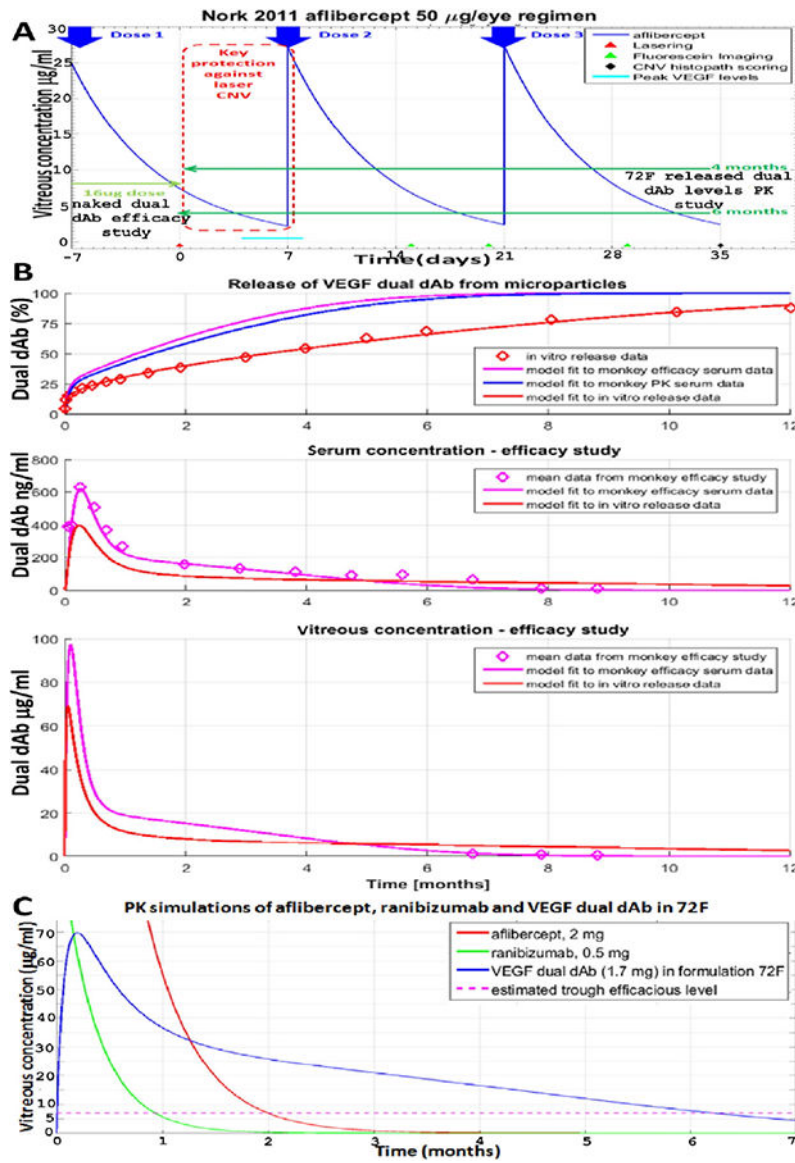


Fig. 6. Modelling long term 72F/dual dAb ocular PK in Cynomolgus and human. (A) Schematic of lowest aflibercept dose preventing Cynomolgus grade IV laser CNV lesions [42], superimposed with mean Cynomolgus dual dAb vitreous levels, after four and six months release, extrapolated from 72F in the PK study, (Fig. 3A, B, C and Table 2), and low dose of naked molecule from the efficacy study, (Fig. 3A), (B) simulation of dual dAb release rate from 72F using, *in vitro* release rate and serum PK in Cynomolgus from both PK (Fig. 3B, Fig. S5D, Table S3) and efficacy studies (Fig. S6, Table S8). Open purple diamonds are data points. (C) Predicted human vitreous PK from a single dose of dual dAb-loaded microparticles (72F), ranibizumab and aflibercept.

Table 1

Characterisation of dual dAb-loaded microparticle.

Formulation	w/p ratio	PSA d(0.5) μm	PolyActive recovery (mg/vial)	Protein loading (mg/vial)	Protein loading (%)	Protein EE (%)	% release 6 mo (12 mo)	% residual 6 mo (12 mo)	% mass-balance 6 mo (12 mo)
72A (1000/70/30)	1.2	63	19.9	4.27	17.7	83	44.5	34.6	79.1
72B (1000/72.5/27.5)	1.2	66	30.6	5.54	15.3	72	94	0	94
72C (1500/70/30)	1.2	64	32.7	7.11	17.9	82	35	59.5	94.5
72D (1000/70/30)	1.35	62	17.7	4.23	19.3	81	54.4	31	85.4
72E (1000/72.5/27.5)	1.35	64	22.6	5.23	18.8	77	86.5	0.1	86.6
72F (1500/70/30)	1.35	64	27.2	7.7	22.1	90	66.1 (83.8)	25.4 (5.1)	91.5 (88.9)

PolyActive formulations are: (PEG length/PEG%age/PBT%age), w/p = water/polymer ratio, PSA = particle size average, protein EE = protein encapsulation efficiency, % release = total cumulative percentage of dual dAb detected from in vitro release, % residual = percentage of dual dAb retained in microparticles, % mass-balance = sum of released and residual dual dAb.

Table 2

Summary of intravitreal dual dAb levels in Cynomolgus after dosing with 72B, 72E and 72F.

Formulation	Dose/eye microparticle in mg (dual dAb in µg)	Intravitreal dual dAb µg/ml phase I day 57 (OS)	Intravitreal dual dAb µg/ml phase I day 71 (OD)	Mean intravitreal dual dAb µg/ml phase I day 113	Mean intravitreal dual dAb µg/ml phase II day 169
72B	7.5 mg (1136 µg)	13.30	17.70	7.95	1.53
72E	6.0 mg (1116 µg)	13.40	11.20	1.69	0.77
72F	Phase I [‡] : 6.0 mg (1304 µg)	2.85 ^{‡,*}	3.72 ^{‡,*}		
	Phase II [§] : 3.0 mg (652 µg)			5.09 [§]	4.03 [§]

[‡]Data from animal I08251, dosed in phase I,

[§]at twice the dose of animals dosed with 72F in phase II.

* intravitreal drug levels should be interpreted with caution, animal I08251 had developed a serum ADA response to dual dAb, (d29) and vitreal ADA was present at d71, (Table S4). For 72B, data is from animal I08245 at d57/71, I08246 (d113) and I08247 (d169); for 72E, data is from animal I08248 at d57/71, I08249 (d113) and I08250 (d169) and for 72F, data is from animal I08251 at d57/71, I08253 (d113) and I08252 (d169), Table S3.

Table 3

Summary of protection against grade IV laser CNV lesions in Cynomolgus (ADA free) by naked and slow-released dual dAb from a single IVT dose.

Group (time of laser)	Number of eyes lasered (separate ADA free animals)	Grade IV lesions/ burn day 14 post laser (%)	Grade IV lesions/ burn day 21 post laser (%)	Statistical analysis by Fischer's exact test <i>P</i> -value, data: (i) day 14, (ii) day 21	Control or test group	Comments
Group 1 empty MPs (day 92)	6	9/54 (16.7%)	10/54 (18.5%)	See Group 2 (day 92 laser)	Negative control	Low lesion number for a negative control
Group 2 72F (day 92)	6	4/54 (7.4%)	5/54 (9.3%)	(i) d14 Group 1 v Group 2, <i>P</i> = 0.236 (ii) d21 Group 1 v Group 2, <i>P</i> = 0.265	Test	3 animals have been excluded as ADA + ve
Group 4 aflibercept (OD) (day 92)	6	21/54 (38.9%)	17/54 (31.5%)	(i) d14 Group 2 v Group 4, <i>P</i> < 0.001 (ii) d21 Group 2 v Group 4, <i>P</i> = 0.008	Negative control	Expected lesion number for a negative control
Group 1 empty MPs (day 148)	6	24/54 (44.4%)	24/54 (44.4%)	See Group 2 (day 148 laser)	Negative control	Expected lesion number for a negative control
Group 2 72F (day 148)	5	5/45 (11.1%)	2/45 (4.4%)	(i) d14 Group 1 v Group 2, <i>P</i> < 0.001 (ii) d21 Group 1 v Group 2, <i>P</i> < 0.001 Effective	Test	1 animal has been excluded as ADA + ve
Group 4 aflibercept (OS) (day 148)	6	0/54 (0%)	0/54 (0%)	(i) d14 Group 1 v Group 4, <i>P</i> < 0.001 (ii) d21 Group 1 v Group 4, <i>P</i> < 0.001 Effective	Positive control	Aflibercept dose at day 141 (OS)
Group 3 * 16 µg dual dAb (day 1)	6	1/54 (1.85%)	1/54 (1.85%)	Effective	Test	+ last 4/6 eyes dosed had inflammation due to LPS contamination
Group 3 \$ 160 µg dual dAb (day 30)	6	0/54 (0%)	0/54 (0%)	Effective	Test	

Eyes were dosed with, Group 1: empty microparticles (MPs), Group 2: dual dAb-loaded microparticles: 72F; Group 3, 2 different doses of naked dual dAb and simultaneously lasered:

* day 1, right eye (OD) 16 µg and

\$ day 30 left eye (OS) 160 µg; Group 4: aflibercept (2 mg), day 1 right eye (OD), day 141 left eye, (OS), Fig. 4A.